BŞEÜ Fen Bilimleri Dergisi
6(2), 629-637, 2019

BSEU Journal of Science
DOI: 10.35193/bseufbd. 613777

e-ISSN: 2458-7575 (http://dergipark.gov.tr/bseufbd)

Araştırma Makalesi - Research Article

Mn katkılı ZnS Nanopartiküllerinin Yapısal ve Optik Özellikleri: Sol-gel ve Kuantum Kimyasal Çalışmaları

Asli Ayten KAYA[1,2*]

Geliş / Received: 01/09/2019 ***Revize / Revised: 27/10/2019*** ***Kabul / Accepted: 05/11/2019***

ÖZ

Bu çalışmada, katkısız ve Mn katkılı ZnS nanopartikülleri (ZnS: Mn), oda sıcaklığında sol-jel yöntemi ile büyütülmüş ve X-ışını kırınım yöntemi ile karakterize edilmiştir. Mn iyonlarının konsantrasyonu % 2-6 arasında değiştirildi. ZnS ince filmlerine Mn katkısının optik özellikleri üzerine etkisi rapor edilmiştir. Bu sonuçlar farklı teknikler ile elde edilen Mn katkılı ZnS ince filmleri ile de karşılaştırıldı. UV-gör. Bölge çalışmalarında, bant boşluğu enerjisi, Mn katkı oranına bağlı olarak 3,45-3,67 eV aralığında bulunmuştur. İlave olarak, katkılı ve Mn katkılı ZnS nanopartiküller küme olarak modellenerek yarı deneysel yöntem ile kuramsal hesaplamaları yapıldı. Bu hesaplamalarda, Zn_7S_7 ve $Zn_5Mn_2S_7$ molekülleri yarı deneysel pm6 seviyesi ile optimize edilmiştir. Her iki molekül için teorik bant boşlukları aynı yöntem ile hesaplanmıştır.

Anahtar Kelimeler- Sol-Gel Yöntemi, Nanopartiküller, İnce Film, PM6

[1,2*] Sorumlu yazar iletişim: asli.kaya@btu.edu.tr (https://orcid.org/0000-0002-2963-6905)
Department of Physics, Bilecik Seyh Edebali University, Bilecik, Turkey.
Department of Physics, Bursa Technical University University, Bursa, Turkey.

BŞEÜ Fen Bilimleri Dergisi
6(2), 629-637, 2019

BSEU Journal of Science
DOI: 10.35193/bseufbd. 613777

e-ISSN: 2458-7575 (http://dergipark.gov.tr/bseufbd)

Structural and Optical Properties of Mn doped ZnS Nanoparticles: Sol-gel and Quantum Chemical Studies

ABSTRACT

In the present work, undoped and Mn-doped ZnS nanoparticles (ZnS:Mn) were growth by the sol-gel method at room temperature and characterized by X-ray diffraction method. The concentration of the Mn ions was changed from 2 to 6%. The influence of Mn doping on the optical properties of un-doped ZnS thin films was reported. These results were also compared to the ZnS:Mn thin films produced by different techniques. In UV-Vis. studies, the band gap energy was found to be 3.45–3.67 eV depending on the Mn doping ratio. In addition, undoped and Mn-doped ZnS nanoparticles were theoretically performed as a cluster by semi empirical calculations. In these calculations, the Zn_7S_7 and $Zn_5Mn_2S_7$ were optimized by semi-empirical pm6 level. The theoretical band gaps for both molecules were calculated with same method.

Keywords- Sol-Gel Process, Nanoparticles, Thin Film, PM6

BŞEÜ Fen Bilimleri Dergisi
6(2), 629-637, 2019

BSEU Journal of Science
DOI: 10.35193/bseufbd. 613777

e-ISSN: 2458-7575 (http://dergipark.gov.tr/bseufbd)

I. INTRODUCTION

The Zinc Sulfide (ZnS) is a II-VI semiconductor with a wide direct band gap in the near UV region. It is an attractive material to be used as an electro-optic modulator, anti-reflecting coating in solar cells, sensors, infrared Windows and lasers [1-5]. There are different thin-film-production techniques to prepare ZnS thin films, such as sol-gel, chemical vapor deposition [6], spray pyrolysis [7], chemical bath deposition [8], electron beam evaporation [9], and successive ionic layer adsorption and reaction (SILAR) [10]. The sol–gel production of films is a quickly progressive technology where the process is based on hydrolysis and condensation reaction of organometallic compounds in alcoholic solutions. This method has been extended to the production of thin films or powder nanoparticles. The sol–gel is the most extensive method for producing nanoparticles due to a low-cost, easy application and homogeneous product.

On the other hand, the cubic zinc blend, hexagonal wurtzite and cubic rock salt polymorphs crystals are observed in ZnS. Each phase has unique physical properties and nonlinear optical coefficients [11-13]. The cubic zinc blend and hexagonal wurtzite phases have industrial applications, and so, it is important to synthesis, characterization, properties such metal oxides. In addition, a low-temperature synthesis of ZnS nanoparticles with hexagonal wurtzite structure has been reported in the literature [14-17]. Theoretical studies on metal oxide nanoparticles have been extensively increased last decades, due to the development of calculation methods. Theoretical calculations have emerged to provide important information regarding the electronic, optic and structural properties of solid materials [18-23], and have presented great value, not only in the interpretation of experiments, but also in the prediction of important aspects of new properties and in the design of new devices.

In this study, undoped and Mn-doped ZnS nanoparticles were synthesized by using sol-gel method and characterized by X-ray diffraction method. Then, the influence of Mn doping on optical properties of ZnS thin films was reported. In addition, theoretical studies were performed for modelling ZnS and Mn-doped ZnS nanoparticles. The ZnS and Mn-doped ZnS nanoparticles were modelled as Zn_7S_7 and Zn_6MnS_7, respectively in theoretical calculation. The structural parameters, band gaps and the frontier molecular orbitals were also investigated.

II. EXPERIMENTAL AND COMPUTATIONAL METHOD

Un-doped and Mn-doped ZnS nanoparticles ($Zn_{1-x}Mn_xS$, x = 0, 0.02, 0.04, 0.06) were obtained by a sol–gel technique using $Zn(Ac)_2$ $2H_2O$, $MnCl_2.4H_2O$ and Na_2S. All chemicals were mixed with the molar equivalent in water solution. The solutions were firstly stirred at 70 °C for 1 h to homogeneous solution and then, heated at 150 °C for several hours for evaporate the solvent, so the powder nanoparticles were obtained. The UV-vis spectra in the range of 350-800 nm were measured using AGILENT - CARY60 model UV–vis Spectrophotometer.

Un-doped and Mn-doped ZnS nanoparticles were modelled as Zn_7S_7 and Zn_6MnS_7 clusters. All clusters were optimized using semiempirical method and pm6 basis set in Gaussian 09 software packed [24]. Preparing the input files and viewing the output files was performed with the Gausview program [25]. Free bonds of the sulphur, zinc and manganese atoms in ZnS clusters have been copulated by hydrogen atoms in order to neutralize the charge of the cluster in the input file. All cluster atoms except terminating hydrogen atoms were relaxed during calculations. In addition, the frequencies of the all molecules were performed to find a local minimum. The Zn_7S_7 cluster was calculated in triplet spin state, while $Zn_5Mn_2S_7$ was performed doublet spin state due to calculate lowest energy value. Geometry optimization, molecular orbital calculations and frontier molecular orbitals, Highest Occupied Molecular Orbital, HOMO and Lowest Unoccupied Molecular Orbital, LUMO were calculated for both clusters.

III. RESULTS AND DISCUSSION

BŞEÜ Fen Bilimleri Dergisi
6(2), 629-637, 2019

BSEU Journal of Science
DOI: 10.35193/bseufbd. 613777

e-ISSN: 2458-7575 (http://dergipark.gov.tr/bseufbd)

The formation of ZnS and Mn-doped ZnS was confirmed by powder X-ray diffraction analysis. Figure 1 shows the XRD patterns of ZnS and %2 Mn-doped ZnS nanocrystals. In Figure 1, the peaks observed in the XRD patterns of ZnS nanoparticles at 2θ values of 28.71, 47.14, 56.17, 69.34 and 77.60° match perfectly with the (111), (220), (311), (400) and (331) crystalline planes of the face centered cubic structure of ZnS. The intensity of diffraction peaks decreases as doped Mn. In both patterns no peaks corresponding to impurities were detected, indicating high purity of the products.

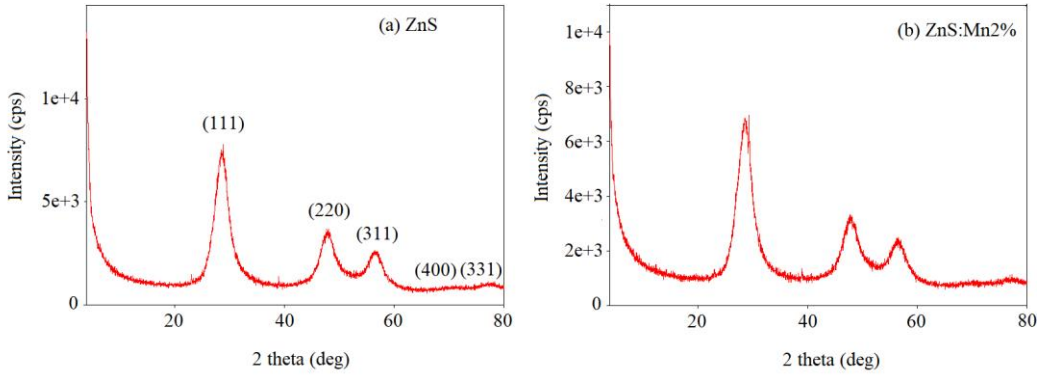

Figure 1. X-ray diffraction (XRD) pattern of (a) ZnS, (b) %2 Mn-doped ZnS nanoparticles

To investigation of optical properties of the un-doped and Mn-doped ZnS nanoparticles, absorbance, transmittance and reflectance spectra were measured with UV-vis spectrophotometer at 350-800 nm, and given in Figure 2. These absorption spectra were used for analyzing band gap energy (Eg). As seen in Figure 2(a), the absorbance values decrease with increasing the wavelength. In addition, it was observed that the absorbance values increased with the addition of Mn doping. Reflectivity properties also show behavior similar to absorbance properties as seen in Figure 2(c).

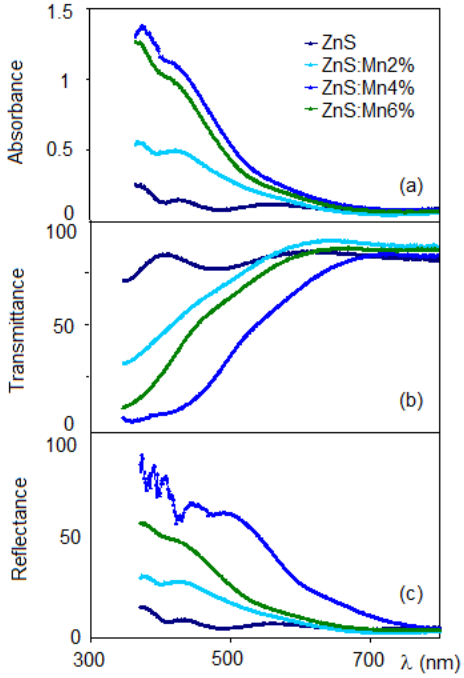

Figure 2. (a) Absorbance, (b) transmittance and (c) reflectance spectra for the un-doped and Mn-doped ZnS nanoparticles

BŞEÜ Fen Bilimleri Dergisi
6(2), 629-637, 2019

BSEU Journal of Science
DOI: 10.35193/bseufbd. 613777

e-ISSN: 2458-7575 (http://dergipark.gov.tr/bseufbd)

It is seen that the transmissions of all nanoparticles decrease with reduction of wavelength except un-doped ZnS. In addition, it can be clearly seen that the transmission decreases of the Mn doping. This decrease may be caused by the addition of manganese causing structural changes in nanoparticles.

The optical band gap, Eg of the un-doped and Mn-doped nanoparticles can be calculated from the absorption spectra using the following formula, which is allowed direct transitions:

$(\alpha h\nu)^2 = A(h\nu - Eg)$

Where α is the absorption coefficient, A is a constant, h is the Planck constant and ν is the frequency of photon. The curves of (αhν)2 versus hν of un-doped and Mn-doped ZnS nanoparticles are given in Figure 3. The Eg value of un-doped ZnS nanoparticle was calculated at 3.67 eV. The optical band gap decreased with Mn doping, and so The Eg values of 2, 4, 6% Mn-doped ZnS were performed as 3.64, 3.51 and 3.45 eV, respectively.

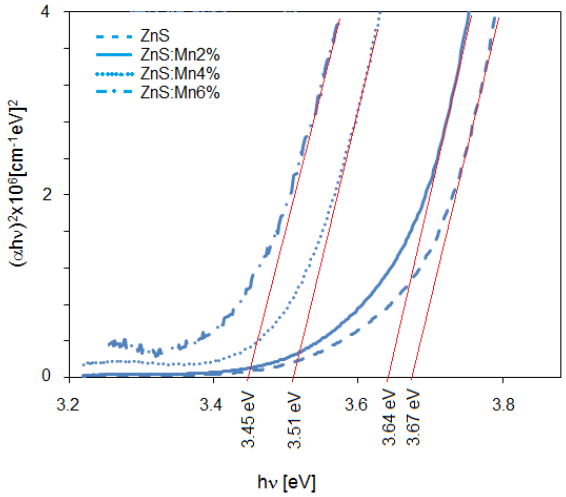

Figure 3. The $(\alpha h\nu)^2$ versus photon energy (hν) for the undoped and Mn-doped ZnS nanoparticles

In this study, firstly, the single point energies of each spin state of Zn_7S_7 and Zn_6MnS_7 clusters were calculated for the most stable spin state. As a result of spin state studies, the lowest energy spin states were determined as triplet state for Zn_7S_7 and doublet state for Zn_6MnS_7. After the appropriate spin states are determined, the Zn_7S_7 and Zn_6MnS_7 clusters were fully reoptimized at semi empirical method and pm6 basis set. The optimized structures of both clusters are given in Figure 4.

BŞEÜ Fen Bilimleri Dergisi
6(2), 629-637, 2019

BSEU Journal of Science
DOI: 10.35193/bseufbd. 613777

e-ISSN: 2458-7575 (http://dergipark.gov.tr/bseufbd)

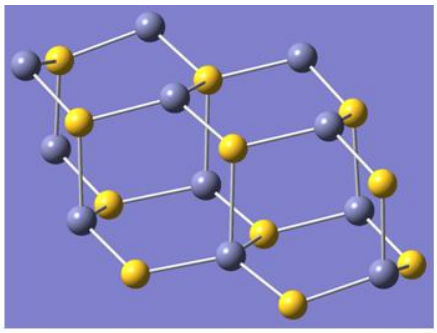

ZnS

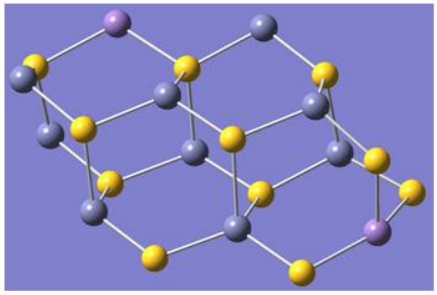

Mn doped-ZnS

Figure 4. The optimized structures of the Zn_7S_7 and Zn_6MnS_7 clusters

The average bond distances and angles of both clusters are listed in Table 1. Zn-S bond lengths in the Zn_7S_7 and Zn_6MnS_7 clusters were calculated average 2.128 and 2.147 Å, respectively. In addition, the Mn-S bond distance in the Zn_6MnS_7 cluster was performed as 2.338 Å. As a result of calculations, the average Zn-S bond was increased with amount of dopant. On the other hand, the average bond angles of the Zn-S-Zn and S-Zn-S were calculated as 110.8° and 113.7°, respectively in the Zn_7S_7 cluster. These bond angles were performed as 108.2° and 111.0°, respectively in the Zn_6MnS_7 cluster. The Mn-S-Zn and S-Mn-S angles of the Zn_6MnS_7 cluster were also calculated at ca. 109.58°.

Table 1. Some bond lengths and angles of the Zn_7S_7 and $Zn_5Mn_2S_7$ clusters.

Cluster	Average bond length (Å)
Zn7S7	
Zn–S	2.128
Zn6MnS7	
Zn–S	2.147
Mn–S	2.338
Bond angles (°)	
Zn7S7	
Zn–S–Zn	110.8
S–Zn–S	113.7
Zn6MnS7	
Zn–S–Zn	108.2
S–Zn–S	111.0
Mn–S–Zn	109.4
S–Mn–S	109.5

Frontier molecular orbitals, which are HOMO and LUMO namely Highest Occupied Molecular Orbital and Lowest Unoccupied Molecular Orbital respectively, are important for determining reactivity of clusters. The

HOMO and LUMO of the Zn_7S_7 and Zn_6MnS_7 clusters were performed using semi empirical/pm6 level and shown in Figure 5. The band gap between HOMO and LUMO is very important for interpretation of stability. The band gap of the Zn_7S_7 was calculated at 3.45 eV, while performed at 2.82 eV for Zn_6MnS_7. The theoretical band gaps were found higher than the experimental values (3.67 eV for un-doped ZnS and 3.64-3.45 eV for doped ZnS). In addition, it has been observed that decreases the band gap value with doping. As seen in Figure 5, the HOMO is situated mainly on Zn atoms in the Zn_7S_7 cluster and Mn atom in the Zn_6MnS_7 cluster, while the electron density localized over Zn and S atoms, Mn and S atoms, respectively in the LUMO orbital for the both clusters.

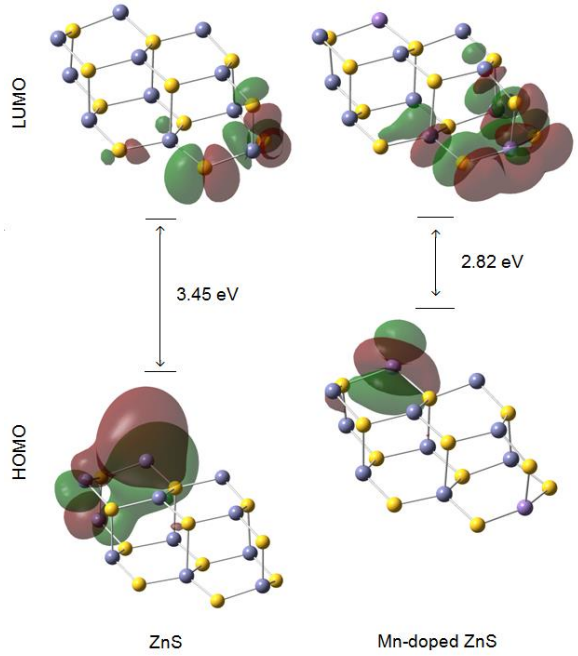

Figure 5. Frontier molecular orbitals and band gaps of the Zn_7S_7 and Zn_6MnS_7 clusters

IV. CONCLUSIONS

The optical properties of the ZnS and Mn-doped ZnS nanoparticles synthesized by sol-gel and characterized by X-ray diffraction methods were performed from UV-vis spectra. In addition, optimized structures and band gaps were calculated by using semi empirical/pm6 level in accordance with experimental values. It was determined that the band gap of ZnS decreased with increasing manganese ratio.

REFERENCES

[1] Ozutok, F. Erturk K. and Bilgin, V. (2012). Growth, Electrical, and Optical Study of ZnS:Mn Thin Films. *Acta Physica Polenica A*, 121, 221-223.

[2] Gómez-Barojas, E. Sánchez-Mora, E. Mendoza-Dorantes, T. Castillo-Abriz, C. and Silva-González, R. (2009). Study of the influence of annealing parameters on the optical and compositional properties of ZnS, ZnS:Mn and ZnS:Sm grown by Sol Gel. *Journal of Physics: Conference Series***,** 167**,** 012051.

[3] Parak, W.J. Gerion, D. Pellegrino, T. Zanchet, D. Micheel, C. Williams, S.C. Boudreau, R. Le Gros, M.A. Larabell, C.A. and Alivisatos, A.P. (2003). Conformation of Oligonucleotides Attached to Gold Nanocrystals Probed by Gel Electrophoresis. *Nano Lett*, 3, 33–36.

[4] Falcony, C. Garcia, M. Ortiz, A. and Alonso, J.C. (1992). Luminescent properties of ZnS:Mn films

deposited by spray pyrolysis. *J Appl Phys*, 72, 1525-1527.

[5] Ding, J.X. Zapien, J.A. Chen, W.W. Lifshitz, Y. Lee, S.T. and Meng, X.M. (2004). Lasing in ZnS nanowires grown on anodic aluminum oxide templates. *Appl Phys Lett*, 85, 2361-2363.

[6] Barreca D., Gasparotto, A. Maragno, C. Tandello, E. and Spalding, T.R. (2002). Analysis of Nanocrystalline ZnS Thin Films by XPS. *Surf. Sci. Spectra* 9, 54-61.

[7] Afifi, H.H. Ashour, A. and Mahmoud, S.A. (1995). Structural study of ZnS thin films prepared by spray pyrolysis. *Thin Solid Films* 263, 248-251.

[8] Nabiyouni, G. Sahraei, R. Toghiany, M. Majles Ara, M.H. and Hedayati, K. (2011). Preparation and characterization of nano- structured ZnS thin films grown on glass and n-type Si substrates using a new chemical bath deposition technique. *Rev. Adv. Mater. Sci.* 27, 52-57.

[9] Wang, S. Fu, X. Xia, G. Wang, J. Shao, J. and Fan, Z. (2006). Structure and optical properties of ZnS thin films grown by glancing angle deposition. *Appl. Surf. Sci.* 252, 8734-8737.

[10] Lindross, S. Kannianen, T. and Leskela, M. (1997). Growth of ZnS thin films by liquid-phase ... highly oriented PbS thin films. *Mater. Res. Bull.* 32, 1631-1636.

[11] Wagner, H. P. K€uhnelt, M. Langbein, W. and Hvam, J. M. (1998). Dispersion of the Second-Order Nonlinear Susceptibility in ZnTe, ZnSe, and ZnS. *Phys. Rev. B*, 58, 10494–501.

[12] Brafman O. and Mitra, S. S. (1968). Raman Effect in Wurtzite- and Zinc-Blende-Type ZnS Single Crystals, *Phys. Rev.*, 171, 931–4.

[13] Ding, Y. Wang, X. D. and Wang, Z. L. (2004). Phase Controlled Synthesis of ZnS Nanobelts: Zinc Blende vs Wurtzite, *Chem. Phys. Lett.*, 398, 32–36.

[14] Huang F. and Banfield, J. F. (2005). Size-Dependent Phase Transformation Kinetics in Nanocrystalline ZnS, *J. Am. Chem. Soc*., 127, 4523–4529.

[15] La Porta, F. A. Ferrer, M. M. Santana, Y. V. B. Raubach, C. W. Longo, V. M. Sambrano, J. R. Longo, E. Andres, J. Li, M. S. and Varela, J. A. (2013).Synthesis of Wurtzite ZnS Nanoparticles Using the Microwave Assisted Solvothermal Method, *J. Alloys Compd*, 555, 153–159.

[16] Tong, H. Zhu, Y. J. Yang, L. X. Li, L. Zhang, L. Chang, J. An, L. Q. and Wang, S. W. (2007). Self-Assembled ZnS Nanostructured Spheres: Controllable Crystal Phase and Morphology. *J. Phys. Chem. C*, 111, 3893–3900.

[17] Feigl, C. A. Barnard, A. S. and Russo, S. P. (2012). Size- and Shape-Dependent Phase Transformations in Wurtzite ZnS Nanostructures. *Phys. Chem. Chem. Phys*., 14, 9871–9879.

[18] Hohenberg P. and Kohn, W. (1964). Inhomogeneous Electron Gas. *Phys. Rev*., 136, B864–B871.

[19] Kohn W. and Sham, L. J. (1965). Self-Consistent Equations Including Exchange and Correlation Effects. *Phys. Rev*., 140, A1133–1138.

[20] Zhao Y. and Truhlar, D. G. (2008). Density Functionals with Broad Applicability in Chemistry, *Acc. Chem. Res.*, 41, 157–167.

[21] Neugebauer J. and Hickel, T. (2013). Density Functional Theory in Materials Science. *WIREs Compt. Mol. Sci.*, 3, 1–11.

[22] Krainara, N. Limtrakul, J. Illas, F. and Bromley, S. T. (2013). Magic Numbers in a One-Dimensional

Nanosystem: ZnS Single-Walled Nanotubes. *J. Phys. Chem. C*, 117, 22908–22914.

[23] Longo, V. M. Gracia, L. Stroppa, D. G. Cavalcante, L. S. Orlandi, M. Ramirez, A. J. Leite, E. L. Andres, J. Beltran, A. Varela, J. A. and Longo, E. (2011). A Joint Experimental and Theoretical Study on the Nanomorphology of CaWO4 Crystals. *J. Phys. Chem. C*, 115, 20113–9.

[24] M.J. Frisch, G.W. Trucks, H.B. Schlegel, G.E. Scuseria, M.A. Robb, J.R. Cheeseman, G. Scalmani, V. Barone, B. Mennucci, G.A. Petersson, H. Nakatsuji, M. Caricato, X. Li, H.P. Hratchian, A.F. Izmaylov, J. Bloino, G. Zheng, J.L. Sonnenberg, M. Hada, M. Ehara, K. Toyota, R. Fukuda, J. Hasegawa, M. Ishida, T. Nakajima, Y. Honda, O. Kitao, H. Nakai, T. Vreven, J.A. Montgomery Jr., J.E. Peralta, F. Ogliaro, M. Bearpark, J.J. Heyd, E. Brothers, K.N. Kudin, V.N. Staroverov, R. Kobayashi, J. Normand, K. Raghavachari, A. Rendell, J.C. Burant, S.S. Iyengar, J. Tomasi, M. Cossi, N. Rega, J.M. Millam, M. Klene, J.E. Knox, J.B. Cross, V. Bakken, C. Adamo, J. Jaramillo, R. Gomperts, R.E. Stratmann, O. Yazyev, A.J. Austin, R. Cammi, C. Pomelli, J.W. Ochterski, R.L. Martin, K. Morokuma, V.G. Zakrzewski, G.A. Voth, P. Salvador, J.J. Dannenberg, S. Dapprich, A.D. Daniels, Ö. Farkas, J.B. Foresman, J.V. Ortiz, J. Cioslowski, D.J. Fox, Gaussian 09, Revision D.01, Gaussian Inc., Wallingford CT, (2009).

[25] Dennington, R. Keith, T. Millam, J. Eppinnett, K. Hovell, W.L. Gilliland, R. (2003). GaussView, Version 3.07, Semichem Inc., Shawnee Mission, KS.